ESTIMATION OF *IN VIVO* HUMAN MYOCARDIAL FIBRE STRAIN BY INTEGRATING DIFFUSION TENSOR AND TAGGED MRI USING FE MODELLING

V.Y. Wang[1], C. Casta[2], P. Croisille[2], P. Clarysse[2], Y-M. Zhu[2], B.R. Cowan[3], A.A. Young[1,3], M.P. Nash[1,4]

[1] Auckland Bioengineering Institute, University of Auckland, New Zealand
[2] Université de Lyon, CREATIS; CNRS UMR5220; Inserm U1044; INSA-Lyon; France.
[3] Centre for Advanced MRI, University of Auckland, New Zealand
[4] Department of Engineering Science, University of Auckland, New Zealand

ABSTRACT

In this study, we propose a methodology to estimate 3D+time maps of left ventricular fibre strain from human structural and dynamic MRI data. A finite element model integrates fibre principal direction throughout the left ventricle from an *ex vivo* human diffusion tensor MRI acquisition and motion from tagged MRI. This combination enables the estimation of fibre strain and its variation throughout the cardiac cycle. The long-term goal of this study is to apply this technique to an atlas of human fibre orientations and to investigate the importance of having subject-specific fibre orientation for fibre strain analysis.

Index Terms— Human cardiac fibre strain, tagged MRI, Diffusion Tensor MRI, FE modelling

1. INTRODUCTION

The beating heart undergoes complex deformations, and understanding the dynamics and mechanics is a very challenging task. MRI tagging has been extensively used to extract *in vivo* myocardial deformation noninvasively. This modality generates grids within the myocardium as temporary material markers, allowing retrieval of motion information throughout the whole cycle. Clinical evaluations of strain have primarily focused on circumferential strain. However, this may be very different to the contraction of the muscle fibres themselves.

Diffusion tensor MRI (DTMRI) has been used to obtain descriptions of the heart fibre architecture of animals and, more rarely, of humans. It therefore provides critical information that can be incorporated into biomechanical models for the understanding of cardiac dynamics. To-date, most of the existing models have used analytical idealised representations of the fibre structure. The purpose of this study was to develop methods to incorporate realistic fibre orientation data to enable non-invasive estimates of the *in vivo* human fibre strains throughout the cardiac cycle. This may provide more specific markers for the evaluation of regional myocardial function, and thus may help to improve detection of mechanical dysfunction of the heart. To this end, tagged and DTMRI data are integrated using a finite element (FE) modelling framework to quantify fibre strain in the human left ventricle (LV).

2. METHODOLOGY

MR imaging was performed at Hospices Civils de Lyon, France, after approval by the Public Prosecutor of the forensic assessment of a new technique performed and before examination of the heart by the forensic pathologist, in compliance with the French national bio-ethical laws.

2.1. Motion Data Extraction

In vivo tagged MR images of a healthy human heart were acquired using a complementary spatial modulation of magnetization (CSPAMM) technique with a Siemens Avanto 1.5T scanner. The data set consisted of 6 long-axis (LA) and 12 short-axis (SA) slices. The imaging parameters for SA tagged images are summarized as follows: 280mm x 280mm x 33% field of view (FOV), 256x84 acquisition matrix, 20° flip angle, TE/TR = 1.3/30.9 ms, 6 pixel tag spacing, 7mm contiguous slice thickness, 24 images per cardiac cycle. LA tags were oriented radially and images were acquired with the following parameters: 280mm x 280mm x 33% FOV, 256x85 acquisition matrix, 20° flip angle, TE/TR=1.3/18.54ms , 6 pixel tag spacing, 7mm slice thickness, 41 frames per cardiac cycle.

To extract the geometric and kinetic information of the human LV, the CSPAMM images were analysed using a 3D interactive image segmentation and tracking software called CIMTag3D [1]. This process started with defining three landmark points that were used to construct a cardiac coordinate system (with the *x*-axis directed from the LV base to apex, *y* directed from the LV centroid to RV centroid, and *z* directed from anterior to posterior). Subsequently, the epi- and endocardial surfaces of the LV were segmented using a guide-point modelling technique, which allowed a pre-defined generic LV FE model to be customised to the specific geometry throughout the cardiac cycle using user-defined *guide-points* (Figure 1 (a)). Figure 1 (b) shows the LV FE model at frame 1 of the cardiac cycle. After

segmenting the surfaces of the LV, the tag lines from the short- and long-axis CSPAMM images were tracked separately with the aid of a non-rigid image registration technique [2] and subsequently used for reconstructing the 3D deformation field of the LV. This 3D displacement information was represented by a set of 3D material points, which was embedded in the 1st (at which the tag lines were laid down in the grid pattern) frame and the displacements for the subsequent (deformed) frames were derived based on the reconstructed 3D motion (Figure 1 (c)). The root-mean-squared (RMS) error for tracking displacement was approximately 0.34 mm [1].

2.2. Fibre Data Extraction

The fibre orientation data used in this study was based on ex vivo DTMR images of a healthy human heart shortly after explantation and less than 24 hours after death. This data was also used to build the first human statistical atlas of the cardiac fibre architecture [3]. The heart was surrounded and filled with hydrophilic and isotonic gel to restore a normal anatomic geometry, after careful removal of any air and mural thrombi. The plastic container was then placed in a 16 elements head coil. Imaging was performed on the same 1.5T scanner, and main MRI parameters of the diffusion weighted EPI sequence (bipolar scheme) are: TE/TR= 69/6500ms, Nex=6 (with polarity alternation), voxel=2*2*2mm3, parallel imaging (grappa factor=2), partial fourier (6/8), base resolution matrix=128, BW=1628 Hz/Px, echo spacing=0.7ms, 12 directions [4]. The myocardial fibre orientation has been shown to correlate with the direction of maximum diffusion of water molecules in the underlying tissue [5]. Therefore, an eigen-analysis was implemented to calculate the principal eigenvector from the measured diffusion tensor at each voxel. The LV surfaces (Figure 2 (a)) were segmented from the images using customised software (CMGUI, www.cmiss.org/cmgui) and used as masks to extract fibre vectors for only the LV myocardium.

2.3. Incorporating Fibre Orientations

The different imaging conditions involved in the tagged and DTMRI data acquisitions (*in vivo* versus *ex vivo*) prevented direct incorporation of fibre data into the LV FE model. To circumvent this, the following steps have been developed to embed *ex vivo* fibre data into the *in vivo* geometric model:

1) construct a transformation model (LVFE-DTI model), which defines the mapping between the *in vivo* and *ex vivo* LV geometries by fitting the LV FE model to the surface contours segmented from the DTMR images (Figure 2 (b));
2) calculate the fibre angle (defined as the helix angle with respect to local circumferential direction) at each voxel within the LV myocardium and phase-unwrap fibre angles based on a pre-defined smooth fibre field that varies linearly across the wall;
3) use nonlinear FE fitting to parameterise a smoothly continuous field of LV fibre angles into the LVFE-DTI geometric model (Figure 2 (c));
4) reverse-map the fitted fibre field, which showed smooth transmural variation, back to the *in vivo* LV FE model using element coordinates as a material coordinate system registered to the anatomy of the heart (Figure 2 (d)). Detailed description on the warpping method can be found in [6].

2.4. Deformation Models

The LV FE models (described in Section 2.1) were created at every time frame of the imaging cycle. The deformation of these LV FE models only provided information on the LV geometric changes as it deformed, but did not represent the mechanical deformation of the LV. To this end, a free-form deformation technique was adopted whereby the LV FE model at frame 1 was fitted to the displacement field of the 3D material points. Firstly, the points were embedded into the reference model (frame 1) so that a local FE material coordinate was assigned to each of the material points. A least-squares optimisation was then set up to minimise the RMS difference of the global coordinates of these material points between the reference state and any deformed state in the cardiac cycle by modifying the nodal parameters of the LV FE model. The fitting was implemented in a customised modelling software CMISS (www.cmiss.org/cm).

2.5. Strain Analysis

Constructing the deformation models enables the evaluation of myocardial strains throughout the cardiac cycle. Of particular interest are the end-systolic (ES) strains. In this study, two strain measures were considered: (1) circumferential strain, which quantifies the strain along the local circumferential direction in the LV short-axis; and (2) fibre strain which quantifies the strain along the local fibre direction. To gain insight into the regional variation of the circumferential and fibre strains at end-systole, strains were evaluated at a set of evenly-spaced points (55438 points) spanning the LV myocardium.

3. RESULTS

Figure 3 illustrates a colour map of the ES circumferential and fibre strains at a uniform grid of points. Figure 4 quantifies the transmural distributions of fibre angles, and circumferential and fibre strains at the same points.

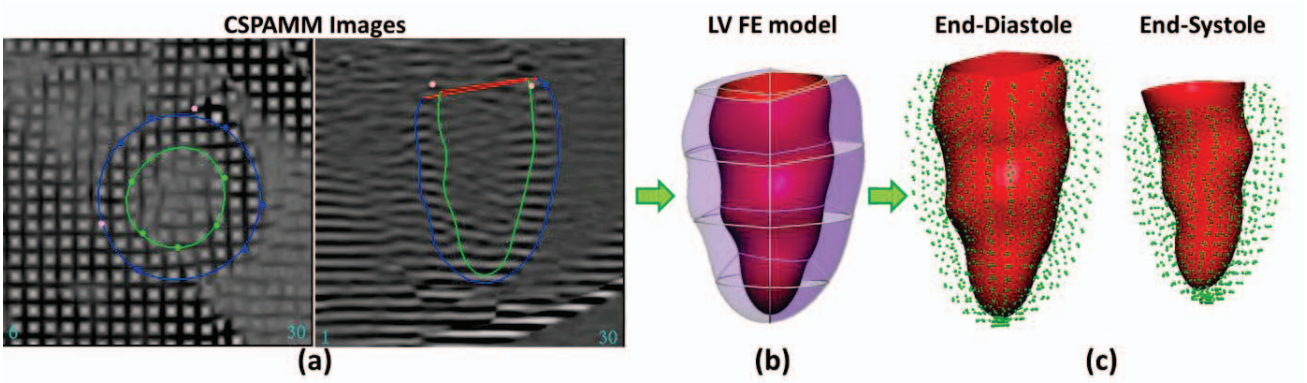


Figure 1: (a) Short- (left) and long-axis (right) CSPAMM images of a healthy human LV with endocardial (green) and epicardial (blue) surface contours and their associated guide-points. (b) LV FE model fitted to the LV CSPAMM image contours at end-diastole. (c) 3D material points derived from tracked tags at the end-diastolic (left) and end-systolic (right) states superimposed with the LV endocardial surfaces (red).

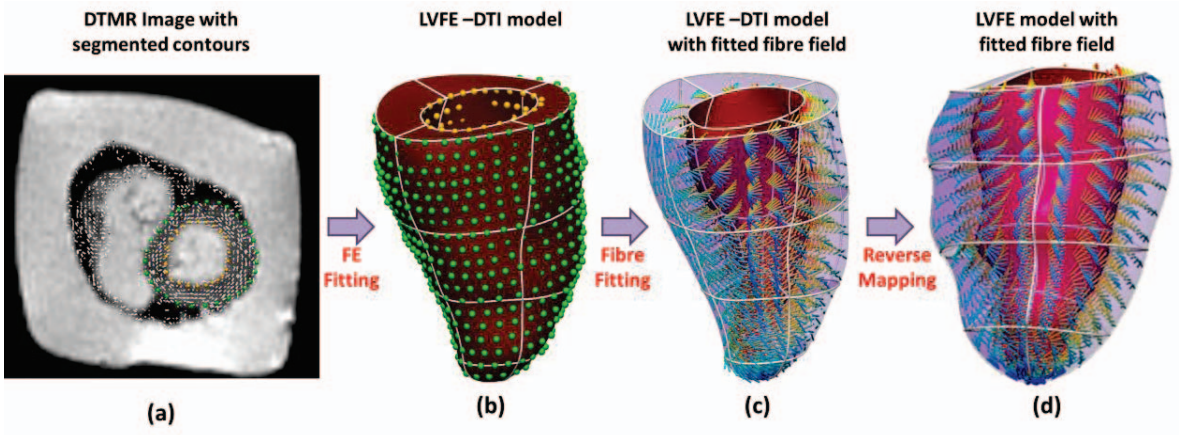


Figure 2: (a) A short-axis DTMR image showing segmented surface contour points (green: epicardial surface; gold: endocardial surface) and myocardial fibre vectors extracted from the diffusion tensor data. (b) The transformation (LVFE-DTI) model used to map geometric information between *in vivo* and *ex vivo* states. (c) LVFE-DTI model with fitted fibre angle field, which was subsequently reverse-mapped back to the *in vivo* LV FE geometric model (d).

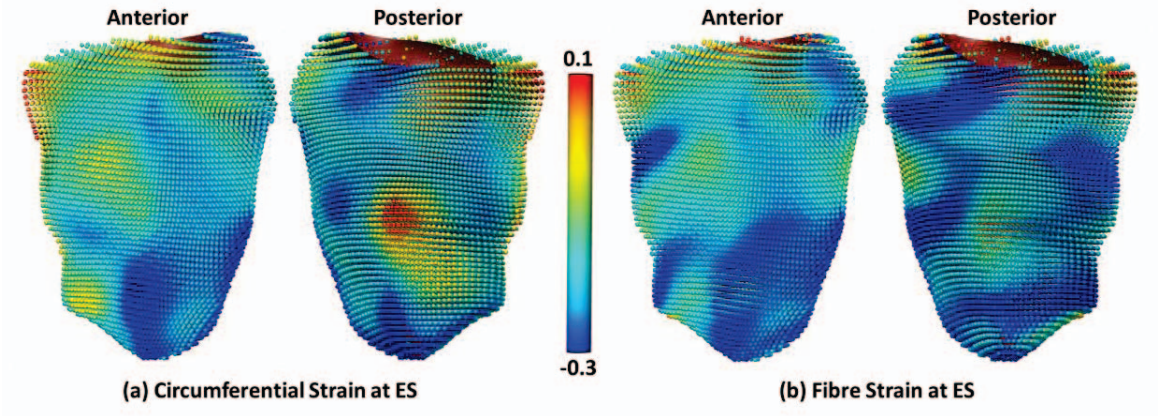


Figure 3: Spatial variation of end-systolic circumferential (a) and fibre (b) strain distributions.

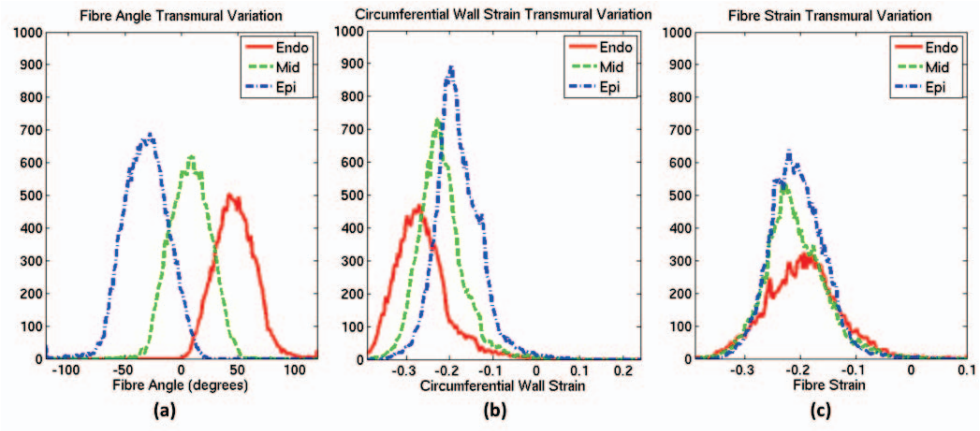


Figure 4: Transmural variations of end-systolic fibre angles (a), circumferential strain (b), and fibre strain (c).

As Figure 4 (a) illustrates, the peak of the histogram shifted from approximately 50° in the endocardium, through approximately 0° in the mid-wall, to -50° in the epicardium. This transmural variation is consistent with previous studies [7]. Similar histograms were generated from the estimates of strain with respect to the circumferential (Figure 4(b)) and fibre (Figure 4 (c)) directions. The ES fibre strains, were approximately normally distributed with similar mean fibre strains of approximately -0.22. This, however, was not the case for the transmural distribution of ES circumferential strain. The mean circumferential strain increased from epicardial to endocardial regions.

4. DISCUSSION AND CONCLUSIONS

The main outcome of this study was the development of a FE modelling framework that integrates myocardial architectural information and motion data to evaluate fibre strains throughout the cardiac cycle. Preliminary data showed that ES fibre strains were approximately homogeneously distributed throughout the ventricular wall. However, this was not the case for the conventional circumferential strain metric, which may be incorrectly interpreted to conclude that endocardial fibres undergo a greater extent of cellular shortening compared to the epicardium during systole. We observed that the ES circumferential strain exhibited a greater degree of spatial variation than the fibre strain (Figure 3). This observation was hypothesised by [8] who used a theoretical modelling framework to optimise fibre orientations to achieve homogeneous fibre strains at ES.

A limitation of this study is that the tagging and DTMRI data were derived from different hearts, since high resolution *in vivo* DTMRI is not currently available. Also, just one set of DTMRI was considered in this study, which raises the question as to whether the use of other DTRMI data will also exhibit homogeneous fibre strain distributions. We are presently extending our analysis to explore the effects of using several different sets of DTMRI data in order to quantify the sensitivity of fibre strain estimates to the variation in human *ex vivo* DTMRI data. Another limitation is the use of just one set of tagged MRI data. To address this, we will consider multiple tagged and DTMRI data sets, and carry out statistical analyses to investigate the inter-subject variation in estimated strain distributions. In the future, an *ex vivo* atlas of human DTMRI may be customised to sparse *in vivo* DTMRI data for evaluation of pathology.

5. REFERENCES

[1] Young A.A., "Model tags: direct 3D tracking of heart wall motion from tagged magnetic resonance images", *Med Image Anal*, 3:361-372, 1999.

[2] Li B., Liu Y., et al. "In-line automated tracking for four dimensional ventricular function with magnetic resonance imaging" *J Am Coll Cardiol Img* 3:860-866, 2010.

[3] Lombaert H., Peyrat J.M., et al. "Statistical Analysis of the Human Cardiac Fiber Architecture from DT-MRI" *FIMH 2011, LNCS 6666*:171–179, 2011.

[4] Frindel C., Robini M., et al. "Comparison of regularization methods for human cardiac diffusion tensor MRI," *Med Image Anal* 13(3):405-418, 2009.

[5] Hsu E.W., Muzikant A.L., et al. "Magnetic resonance myocardial fiber-orientation mapping with direct histological correlation" *Am J Physiol* 275:H1627-1634, 1998.

[6] Wang V.Y., Lam H.I., et al. "Modelling passive diastolic mechanics with quantitative MRI of cardiac structure and function" *Med Image Anal*, 13:773-784, 2009.

[7] Nielsen P.M.F., Le Grice I.J., et al. "Mathematical model of geometry and fibrous structure of the heart" *Am J. Physiol* 260(4):H1365-H1378, 1991.

[8] Rijcken J., Bovendeerd P.H.M., et al. "Optimization of cardiac fiber orientation for homogeneous strain during ejection" *Ann. Biomed. Eng.* 27(3):289-297, 1999.